ABS Design and Active Suspension Control Based on HOSM

Juan Diego Sánchez-Torres, Alejandra Ferreira de Loza, Marcos I. Galicia and Alexander G. Loukianov

***Abstract*— This paper tackles the control of a brake assisted with an active suspension. The goal of the paper is ensure an effective braking process improving the vehicle safety in adverse driving conditions. To address this, the wheel slip ratio is kept to a desired value reducing the effective braking distance by designing of a robust tracking controller based on high order sliding modes algorithms, imposing the anti-lock brake system feature. On the other hand, the active suspension problem is carried with a nested backward sliding surface design. The purpose of this control is to improve the driving comfort. To this aim, the designed controller compensate the effects of the unmatched perturbation coming from the road. This controller exploits a high order sliding modes observer, which guarantees theoretically exact state and perturbation estimation. In both cases, a continuous control action drives the state trajectories to the designed sliding manifolds and keeps them there in spite of the matched and unmatched perturbations. The feasibility of the proposed scheme has been exposed via simulations.**

I. INTRODUCTION

The aim of this paper is to propose robust controllers based on sliding mode (SM) algorithms for a brake coupled with an active suspension. The main difficulties of controller design in automotive systems are related to high non-linearities, uncertainties caused by external perturbations and parameter variations which are unknown. In order to deal with these problems, several researchers have proposed robust control approaches, including those based on SM algorithms [1], [2], [3] and, [4]; considering the problem of ABS design with extremum seeking controllers in order to maximize the tire/road friction [5] and, the analysis of the nonlinear dynamics on these systems [6]. Similarly, there are solutions for the active suspension case [7]. For the case of the ABS and active suspension as a whole system, a backstepping design is presented in [8]; however, for this case the road disturbances are assumed to be known in order to facilitate the control law design. Also for the whole system, in [9] a SM controller with a sliding manifold designed using geometric decoupling methods to disturbance rejection, was proposed.

The SM algorithms, are proposed with the idea to drive the dynamics of a system to a sliding manifold, that is an integral manifold with finite reaching time [10]; exhibiting features such as finite time convergence, robustness to uncertainties and insensitivity to external bounded disturbances [11].

This work was supported by the National Council of Science and Technology (CONACYT), Mexico, under Grant 129591

Juan Diego Sánchez-Torres, Marcos I. Galicia and Alexander G. Loukianov are with Automatic Control Laboratory, CINVESTAV-IPN Guadalajara, Av. del Bosque 1145 Col. El Bajío CP 45019, México, [dsanchez,mgalicia,louk]@gdl.cinvestav.mx

A. Ferreira de Loza is with University of Bordeaux, IMS-Lab, Automatic Control Group, 351 Cours de la Libération, 33405 Talence, France, da_ferreira@yahoo.com

In this work, a controller design for an ABS assisted with an active suspension. Taking advantage of the SM algorithms features, the brake controller is proposed such that it imposes the *anti-lock brake system* ABS property in finite time in spite of perturbations. The ABS forces a desired vehicle motion and, as a consequence, its stability. Similarly, the active suspension is controlled with the objective of guaranteeing the ride quality and comfort for the passengers by reducing the vibration due to the road shape.

These controllers are based on the application of high order sliding modes (HOSM) algorithms [12]. The use of these methods allows the design of robust controllers in presence of external disturbances and parametric variations, which are supposed to be unknown but with a known bound. The main feature of the proposed controllers is the characteristic of exact finite time rejection of both, the matched and the unmatched perturbations, improving the safety and the comfort of the vehicle.

To assess the performance of the designed controllers, the closed loop system is tested by means of numerical simulation.

In the following, Section II presents the considered model. Sections III and IV describe the proposed controllers for the ABS and active suspension problems, including a detailed analysis of stability and robustness. The successful simulations are presented in section V. Finally, in Section VI the conclusions are given.

II. MATHEMATICAL MODEL

In this section, we consider a quarter of vehicle model, this model includes the active suspension, the pneumatic brake system, the wheel motion and the longitudinal vehicle motion.

A. Active Suspension Model

The quarter-car active suspension is a 2-DOF mechanical system shown in Fig. 1.

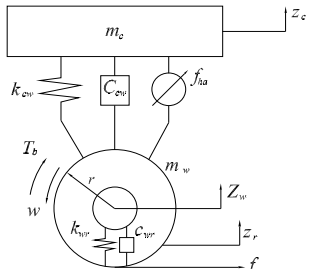

Fig. 1. Active suspension scheme.

This system connects the car body and the wheel masses and is modeled as a linear viscous damper and a spring

elements, whereas the tire is represented as a linear spring and damping elements. The motion equations for this system are given by

$$\begin{aligned} m_c\ddot{z}_c &= -K_{cw}\left(z_c - z_w\right) - C_{cw}\left(\dot{z}_c - \dot{z}_w\right) + f_{ha} \\ m_w\ddot{z}_w &= K_{cw}\left(z_c - z_w\right) + C_{cw}\left(\dot{z}_c - \dot{z}_w\right) \\ &\quad -K_{wr}\left(z_w - z_r\right) - C_{wr}\left(\dot{z}_w - \dot{z}_r\right) - f_{ha} \end{aligned} \tag{1}$$

where m_c and m_w are the mass of the car and the wheel, respectively, z_c is the car vertical displacement, z_w is the wheel vertical displacement, K_{cw} and K_{wr} are the spring coefficients, C_{cw} and C_{wr} are the damping coefficients, f_{ha} is the force of the hydraulic actuator, z_r is the disturbance due to road and $\dot{z}_r$ is its time derivative.

B. Pneumatic Brake System Equations

The specific configuration of this system considers the brake disk, which holds the wheel, as a result of the increment of the air pressure in the brake cylinder. The entrance of the air trough the pipes from the central reservoir and the expulsion from the brake cylinder to the atmosphere is regulated by a common valve. The time response of the valve is considered small, compared with the time constant of the pneumatic system.

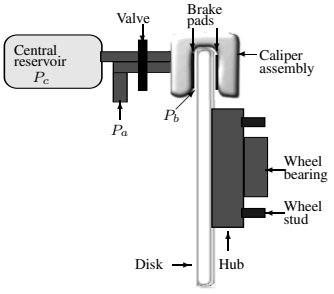

Fig. 2. Pneumatic brake scheme.

Considering Fig. 2, we suppose the brake torque T_b is proportional to the pressure P_b in the brake cylinder

$$T_b = k_b P_b \tag{2}$$

with $k_b > 0$. For the brake system we use an approximated model of pressure changes in the brake cylinder due to the opening of the valve with a first order relation [13], this relation can be represented as

$$\tau\dot{P}_b + P_b = P_c \tag{3}$$

where τ is the time constant of the pipelines, P_c is the pressure inside the central reservoir. The atmospheric pressure, P_a, is considered equal to zero.

C. Wheel Motion Equations

To describe the wheels motion, a partial mathematical model of the dynamic system is used [14]. The dynamics of the angular momentum variation relative to the rotation axis, are given by

$$J\dot{\omega} = -rf\left(s\right) - b_b\omega - T_b \tag{4}$$

where ω is the wheel angular velocity, J is the wheel inertia moment, r is the wheel radius, b_b is a viscous friction coefficient due to wheel bearings and $f(s)$ is the contact force of the wheel.

The expression for longitudinal component of the contact force in the motion plane is

$$f\left(s\right) = \mu f_m \phi\left(s\right) \tag{5}$$

where μ is the nominal friction coefficient between the wheel and the road, f_m is the normal reaction force in the wheel

$$f_m = mg + \Delta f_m(z_r, \dot{z}_r) \tag{6}$$

with m equal to the mass supported by the wheel, g is the gravity acceleration and $\Delta f_m(z_r, \dot{z}_r) = -K_{wr}(z_w - z_r) - C_{wr}(\dot{z}_w - \dot{z}_r)$ represents the variation of normal reaction force due to road perturbation. The function $\phi(s)$ represents a friction/slip characteristic relation between the tire and road surface. Here, we use the Pacejka model [15], [16], defined as follows

$$\phi\left(s\right) = D\sin\left(C\arctan\left(Bs - E\left(Bs - \arctan\left(Bs\right)\right)\right)\right).$$

The slip rate s is defined as

$$s = \frac{v - r\omega}{v} \tag{7}$$

where v is the longitudinal velocity of the wheel mass center. The equations (2)-(7) characterize the wheel motion.

D. The Vehicle Motion Equation

The vehicle longitudinal dynamics without lateral motion is considered. The main reasons for this assumptions are that the steering angle changing has virtually no effect on the force vectors on the wheels. Then, the vehicle longitudinal dynamics is written as

$$M\dot{v} = -F\left(s\right) - F_a(v) \tag{8}$$

where M is the vehicle mass, $F_a(v)$ is the aerodynamic drag force, which is proportional to the vehicle velocity and is defined as

$$F_a(v) = \frac{1}{2}\rho C_d A_f\left(v + v_w\right)^2 + \Delta v_w$$

where ρ is the air density, C_d is the aerodynamic coefficient, A_f is the frontal area of vehicle, v_w is the wind velocity and Δv_w represents its variations.

As in the expression for longitudinal component of the contact force in the motion plane (5), the contact force of the vehicle $F(s)$ is modeled of the form

$$F\left(s\right) = \mu\phi\left(s\right) f_M \tag{9}$$

where μ is the nominal friction coefficient between the wheel and the road, f_M is the normal reaction force of the vehicle

$$f_M = Mg + \Delta f_M(z_r, \dot{z}_r) \tag{10}$$

with M equal to the vehicle mass, g is the gravity acceleration and $\Delta f_M(z_r, \dot{z}_r) = -K_{wr}(z_w - z_r) - C_{wr}(\dot{z}_w - \dot{z}_r)$ represents the variation of normal reaction force due to road perturbation.

E. State Space Equations

The dynamic equations of the whole system (3)-(8) rewritten using the state variables $\mathbf{x} = \begin{bmatrix} x_1 & x_2 & x_3 & x_4 & x_5 & x_6 & x_7 \end{bmatrix}^T = \begin{bmatrix} z_c & \dot{z}_c & z_w & \dot{z}_w & \omega & P_b & v \end{bmatrix}^T$ results in the following form:

$$\begin{cases} \dot{x}_1 = & x_2 \\ \dot{x}_2 = & -a_1(x_1 - x_3) - a_2(x_2 - x_4) + b_1 u_s \\ \dot{x}_3 = & x_4 \\ \dot{x}_4 = & a_3(x_1 - x_3) + a_4(x_2 - x_4) - a_5 x_3 \\ & -a_6 x_4 - b_2 u_s + \Delta_r \end{cases} \tag{11}$$

$$\begin{cases} \dot{x}_5 = & -a_7 x_5 - a_8 f(s) - a_9 x_6 + \bar{\Delta}_1 \\ \dot{x}_6 = & -a_{10} x_6 + b_3 u_b + \bar{\Delta}_2 \\ \dot{x}_7 = & -a_{11} F(s) - f_w(x_7) + \bar{\Delta}_3 \end{cases} \tag{12}$$

with the outputs

$$y_s = \begin{bmatrix} x_1 & x_3 \end{bmatrix} \text{ and } y_b = \begin{bmatrix} x_5 & x_7 \end{bmatrix}$$

where $a_1 = K_{cw}/m_c$, $a_2 = C_{cw}/m_c$, $a_3 = K_{cw}/m_w$, $a_4 = C_{cw}/m_w$, $a_5 = K_{wr}/m_w$, $a_6 = C_{wr}/m_w$, $a_7 = b_b/J$, $a_8 = r/J$, $a_9 = k_b/J$, $a_{10} = 1/\tau$, $a_{11} = 1/M$, $b_1 = 1/m_c$, $b_2 = 1/m_w$, $b_3 = 1/\tau$, $u_s = f_{ha}$, $u_b = P_c$ and $f_w(x_7) = \frac{1}{2M}(\rho C_d A_f)(x_7 + v_w)^2$.

Here, $\Delta_r = a_5 z_r + a_6 \dot{z}_r$, the term $\bar{\Delta}_1$ contains the variations of the friction parameters μ, b_b, wheel inertia moment J and the normal reaction force due to road perturbation $\Delta f_m(z_r, \dot{z}_r)$. The term $\bar{\Delta}_2$ contains the variations of the parameters τ and P_c. Finally, the term $\bar{\Delta}_3$ contains the variations of the parameters μ, C_d, A_f, ρ, the wind velocity variation Δv_w and the force due to road perturbation $\Delta f_M(z_r, \dot{z}_r)$.

III. ACTIVE SUSPENSION CONTROLLER DESIGN

In this section, a HOSM observer to estimate the state and identify the unknown inputs in finite time is used. Then, a sliding manifold is designed such that the system's motion along the manifold meets the regulation of the system state and the rejection of perturbations coming from the road.

Define $x_s = \begin{bmatrix} x_1 & x_2 & x_3 & x_4 \end{bmatrix}^T$, then the subsystem (11) is represented of the form

$$\begin{aligned} \dot{x}_s &= A_s x_s + B_s u_s + D_s \Delta_r \\ y_s &= C_s x_s \end{aligned} \tag{13}$$

where $A_s = \begin{bmatrix} 0 & 1 & 0 & 0 \\ -a_1 & -a_2 & a_1 & a_2 \\ 0 & 0 & 0 & 1 \\ a_3 & a_4 & -a_3 - a_5 & -a_4 - a_6 \end{bmatrix}$, $B_s = \begin{bmatrix} 0 & b_1 & 0 & -b_2 \end{bmatrix}^T$, $C_s = \begin{bmatrix} 1 & 0 & 1 & 0 \end{bmatrix}$ and, $D_s = \begin{bmatrix} 0 & 0 & 0 & 1 \end{bmatrix}^T$.

Assuming that there is a constant Δ_r^+ such that the perturbation as well as its successive derivatives are bounded, i.e. $|\Delta_r| \leq \Delta_r^+$, $\left|\dot{\Delta}_r\right| \leq \Delta_r^+$, $\left|\ddot{\Delta}_r\right| \leq \Delta_r^+$ for all $t \geq 0$. An algebraic HOSM observer is proposed in order to estimate the state and identify the perturbation. Next subsection is devoted to summarize the observer design, for further details see [17].

A. State Observation and Unknown Input Identification

For estimation purposes system (13) is strongly observable or equivalently for $u_s = 0$ the triplet (A_s, D_s, C_s) has no zeros. Consequently, the state estimation can be achieved from the output and its derivatives. Beforehand the estimation error must be bounded. Consider the following auxiliary system:

$$\dot{\tilde{x}}_s = A_s \tilde{x}_s + B_s u_s + L(y_s - \tilde{y}_s) \tag{14}$$

where $\tilde{y}_s = C_s \tilde{x}_s$ and $\tilde{x}_s$ is the estimate of x_s, matrix L must be designed such that the matrix $\tilde{A} := (A_s - LC_s)$ is Hurwitz. Defining the error $x_e := x_s - \tilde{x}_s$, from (13)-(14) it follows:

$$\dot{x}_e = \tilde{A} x_e + D_s \Delta_r. \tag{15}$$

Thus, the error $x_e(t)$ is ultimately bounded, i.e., there exist a known constant $\delta_e > 0$ and a finite time t_e, such that $\|x_e(t)\| \leq \delta_e$, for all $t > t_e$.

Defining the output of the linear error system $y_e := y_s - \tilde{y}_s$, let us construct an extended vector considering the output vector and the derivative of a linear combination of the output unaffected by the perturbations, i.e.

$$\begin{bmatrix} \frac{d}{dt}(C_s D_s)^{\perp} y_e \\ y_e \end{bmatrix} = \underbrace{\begin{bmatrix} (C_s D_s)^{\perp} C_s \tilde{A} \\ C_s \end{bmatrix}}_{M_s} x_e. \tag{16}$$

Due to the strongly observability property of the system (13), it can be shown that matrix M_s has full rank (see, e.g., [18]). This means that the algebraic equation (16) has a unique solution for x_e. Hence, rearranging the previous equation and pre-multiplying both sides by $M_s^+ := \left(M_s^T M_s\right)^{-1} M_s^T$ it yields to

$$x_e = \underbrace{\frac{d}{dt} M_s^+ \begin{bmatrix} (C_s D_s)^{\perp} C_s \tilde{A} & 0 \\ 0 & I_2 \end{bmatrix} \begin{bmatrix} y_e \\ \int y_e \end{bmatrix}}_{Y_s}. \tag{17}$$

Following [19], under the boundedness assumption of $\left|\ddot{\Delta}_r\right| \leq \Delta_r^+$ a third order sliding mode differentiator can be constructed

$$\begin{aligned} \dot{\nu}_0 &= -5\Lambda^{\frac{1}{3}} \Psi^{\frac{2}{3}}(\nu_0 - Y_s) + \nu_1 \\ \dot{\nu}_1 &= -3\Lambda^{\frac{1}{2}} \Psi^{\frac{1}{2}}(\nu_1 - \dot{\nu}_0) + \nu_2 \\ \dot{\nu}_2 &= -1.5\Lambda^{\frac{1}{2}} \Psi^{\frac{1}{2}}(\nu_2 - \dot{\nu}_1) + \nu_3 \\ \dot{\nu}_3 &= -1.1\Lambda \Psi^0(\nu_3 - \dot{\nu}_2) \end{aligned} \tag{18}$$

where $\nu_i \in \mathbb{R}^2$ for $i = 0, \ldots, 3$ are the outputs of the differentiator, the function vector is defined as $\Psi^k(v_i) = \begin{bmatrix} |v_{1,i}|^k \operatorname{sign}(v_{1,i}) & |v_{2,i}|^k \operatorname{sign}(v_{2,i}) \end{bmatrix}^T$ with $k \in \mathbb{R}$ and Λ is a Lipschitz constant of function $\ddot{Y}_s$ and can be figured from (15) as $\Lambda \geq \left\|\tilde{A}\right\|^2 e^+ + \left\|\tilde{A} D_s + D_s\right\| \Delta_r^+$.

In [19] it was shown that there is a finite time t_f such that the identity $\nu_i = \frac{d^i}{dt^i} Y_s$ is achieved for every $i = 0, \ldots, 3$.

The vector x_e can be reconstructed from the first sliding dynamics, i.e. $\nu_1 = x_e$ accordingly

$$\hat{x} := \nu_1 + \tilde{x} \text{ for all } t \geq t_f$$

where $\hat{x}$ represents the estimated value of x. Therefore, the identity $\hat{x} \equiv x$, for all $t \geq t_f$ holds.

Thus, for identifying the unknown inputs, from (18) we can recover $\dot{x}_e$, i.e. $\nu_2 = \dot{x}_e$ for all $t \geq t_f$ and from (15) it follows that

$$\hat{\Delta}_r := -D_s^+ \left[\tilde{A}\nu_1 - \nu_2\right] \text{ for all } t \geq t_f$$

and consequently calculating the derivative of (15) it yields to

$$\dot{\hat{\Delta}}_r := -D_s^+ \left[\tilde{A}\nu_2 - \nu_3\right] \text{ for all } t \geq t_f$$

where $\hat{\Delta}_r$ and $\dot{\hat{\Delta}}_r$ represent the estimated values of Δ_r and $\dot{\Delta}_r$. Therefore, the identities $\hat{\Delta}_r \equiv \Delta_r$ and $\dot{\hat{\Delta}} \equiv \dot{\Delta}_r$ are fulfilled for all $t \geq t_f$.

B. Nested Backward Sliding Control

Applying twice the regular form [20], the system (13) is transformed into $\bar{x}_{11} = x_1 + \frac{b_1}{b_2}x_3$, $\bar{x}_{12} = x_2 + a_r x_3 + \frac{b_1}{b_2}x_4$, $\bar{x}_2 = x_3$ and, $\bar{x}_3 = x_4$. Where $a_r = -a_2 + \frac{b_1}{b_2}(a_4 + a_6 - a_2) + a_4\left(\frac{b_1}{b_2}\right)^2$ and the transformed system yields to

$$\dot{\bar{x}}_1 = A_1\bar{x}_1 + B_1\bar{x}_2 + D_1\Delta_r \tag{19}$$

$$\dot{\bar{x}}_2 = A_{21}\bar{x}_1 + A_{22}\bar{x}_2 + \bar{x}_3 + D_2\Delta_r \tag{20}$$

$$\dot{\bar{x}}_3 = A_{31}\bar{x}_1 + A_{32}\bar{x}_2 + A_{33}\bar{x}_3 + u_s + D_3\Delta_r \tag{21}$$

where $\bar{x}_1 \in \mathbb{R}^2$, $\bar{x}_2$, $\bar{x}_3 \in \mathbb{R}$, and the matrices are of the corresponding dimensions. Since the system (19) satisfies the matching condition $\text{span}\{D_1\} \subset \text{span}\{B_1\}$, there exist a matrix Γ such that $B_1\Gamma = D_1$, [21]. To this end $\bar{x}_2$ can be exploited and regarded as an input $\bar{x}_2 = -K\bar{x}_1 - \Gamma\hat{\Delta}_r$ then $\dot{\bar{x}}_1 = (A_1 - B_1K)\bar{x}_1$.

In the ideal case $\hat{\Delta}_r \equiv \Delta_r$ and $D_1\left(\Delta_r - \hat{\Delta}_r\right) = 0$. The gain K is designed such that $\bar{A}_1 := A_1 - B_1K$ is Hurwitz. With this aim, let us design the auxiliary variable $\xi = \bar{x}_2 + K\bar{x}_1 + \Gamma\hat{\Delta}_r$ and from (19)-(20) it yields to

$$\begin{aligned} \dot{\bar{x}}_1 &= \bar{A}_1\bar{x}_1 + B_1\xi \\ \dot{\xi} &= \bar{A}_{21}\bar{x}_1 + \bar{A}_{22}\xi_2 + \bar{D}_2\hat{\Delta}_r + \Gamma\dot{\hat{\Delta}}_r + \bar{x}_3 \end{aligned} \tag{22}$$

where $\bar{A}_{21} = A_{21} - A_{22}K - K\bar{A}_1$, $\bar{A}_{22} = A_{22} + KB_1$, $\bar{D}_2 = D_2 - A_{22}\Gamma$.

Now, $\bar{x}_3$ will be designed to stabilize (22). Consider a Lyapunov candidate function $V(\bar{x}_1, \xi) = \bar{x}_1^T P\bar{x}_1 + \xi^T\xi$, where P is a symmetric positive definite matrix satisfying $P\bar{A} + \bar{A}^T P = -I$. Thus, designing

$$\bar{x}_3 = -\left(\left(\bar{A}_{21} + B_1^T P\right)\bar{x}_1 + \left(\bar{A}_{22} + I\right)\xi + \bar{D}_2\hat{\Delta}_r + \Gamma\dot{\hat{\Delta}}_r\right) \tag{23}$$

yields to $\dot{V} \leq -\|\bar{x}_1\|^2 - \|\xi\|^2$. In the ideal case, the coordinates $\bar{x}_1$, ξ will be exponentially stable. Finally, the coordinate $\bar{x}_1$ is exponentially stable, i.e. there exist constants α_1, $\alpha_2 > 0$ such that $\|\bar{x}_1\| \leq \alpha_1 \|\bar{x}_1(0)\| \exp^{-\alpha_2 t}$ for all $t > t_r$, with $t_r > 0$, and the remaining trajectories will be bounded, i.e. $|\bar{x}_2| \leq |K\bar{x}_1| + |\Gamma|\Delta_r^+$ and from (23) there exist some $\Phi > 0$, such that $|\bar{x}_3| \leq \Phi|\bar{x}| + \left|\Gamma + \bar{D}_2\right|\Delta_r^+$ for all $t > t_r$.

Considering (23), the sliding manifold takes the form

$$\sigma = \bar{x}_3 + \varphi\left(\bar{x}_1, \bar{x}_2, \hat{\Delta}_r, \dot{\hat{\Delta}}_r\right) \tag{24}$$

where $\varphi\left(\bar{x}_1, \bar{x}_2, \hat{\Delta}_r, \dot{\hat{\Delta}}_r\right)$ is the nested backward compensator [22], given by $\varphi\left(\bar{x}_1, \bar{x}_2, \hat{\Delta}_r, \dot{\hat{\Delta}}_r\right) = \left(\bar{A}_{21} + B_1^T P + \left(\bar{A}_{22} + I\right)K\right)\bar{x}_1 + \left(\bar{A}_{22} + I\right)\bar{x}_2 + \left(\bar{D}_2 + \left(\bar{A}_{22} + I\right)\Gamma\right)\hat{\Delta}_r + \Gamma\dot{\hat{\Delta}}_r$.

The dynamics of the sliding variable (24) is given by

$$\begin{aligned} \dot{\sigma} = {} & A_{31}\bar{x}_1 + A_{32}\bar{x}_2 + A_{33}\bar{x}_3 + D_3\Delta_r + u_s \\ & + \dot{\varphi}\left(\bar{x}_1, \bar{x}_2, \hat{\Delta}_r, \dot{\hat{\Delta}}_r\right). \end{aligned} \tag{25}$$

To induce SM on the manifold $\sigma = 0$, the super-twisting control algorithm [12] is applied to (25)

$$u_s = u_{s_1} + u_{s_2} \tag{26}$$

with $u_{s_1} = -\left(A_{31}\bar{x}_1 + A_{32}\bar{x}_2 + A_{33}\bar{x}_3 + D_3\hat{\Delta}_r\right)$ $-k_{s_1}|\sigma|^{1/2}\text{sign}(\sigma)$, $\dot{u}_{s_2} = -k_{s_2}\text{sign}(\sigma)$ and $k_{s_1}, k_{s_2} > 0$.

The stability condition for the system (25) closed-loop by (26), can be obtained via the transformation $q_s = u_{s_2} + \varphi\left(\bar{x}_1, \bar{x}_2, \hat{\Delta}_r, \dot{\hat{\Delta}}_r\right)$ to

$$\begin{aligned} \dot{\sigma} &= -k_{s_1}|\sigma|^{\frac{1}{2}}\,\text{sign}(\sigma) - q_s \\ \dot{q}_s &= -k_{s_2}\text{sign}(\sigma) + \dot{\varphi}\left(\bar{x}_1, \bar{x}_2, \hat{\Delta}_r, \dot{\hat{\Delta}}_r\right). \end{aligned} \tag{27}$$

Under the assumption $\left|\dot{\varphi}\left(\bar{x}_1, \bar{x}_2, \hat{\Delta}_r, \dot{\hat{\Delta}}_r\right)\right| < \delta_\varphi < \infty$ and choosing $k_{s_1} > 0$ and $k_{s_2} > 3\delta_\varphi + 4\left(\frac{\Sigma}{k_{s_1}}\right)^2$ then $(\sigma, q_s) = (0, 0)$ in finite time [23]. Establishing a SM in the manifold $\sigma = 0$.

IV. BRAKE CONTROLLER

Consider the brake subsystem (12), defining $x_b = \begin{bmatrix} x_5 & x_6 & x_7 \end{bmatrix}^T$, and taking into account the slip equation (7), the direct action of the pressure P_b in the brake cylinder over the wheels motion, and the measurements of $y_b = \begin{bmatrix} x_5 & x_7 \end{bmatrix}$, the tracking error e_1 is defined as

$$e_1 \triangleq x_5 - \frac{1 - s^*}{r}x_7. \tag{28}$$

Note that if $e_1 = 0$, then $s = s^*$. This results in the maximum friction force, minimizing the braking time until the wheel locking is avoided.

Straightforward calculations reveal that it is possible to write x_5 and x_7 in terms of e_1. From (11), (12) and (28) the dynamics of e_1 can be written in the *Nonlinear Block Controllable* with perturbation form [24]

$$\dot{e}_1 = f_1(e_1) + b_1(e_1)x_6 + \Delta_1(e_1, t) \tag{29}$$

$$\dot{e}_2 = -a_{10}e_2 + b_3u_b + \Delta_2(e, t) \tag{30}$$

where $e_2 = x_6 - x_{6\delta}$ is an auxiliary error variable, with x_6 considered as a virtual control for (29), with desired value $x_{6\delta}$. The expressions $f_1(e_1)$ and $b_1(e_1)$ are given by $f_1(e_1) = \frac{1-s^*}{r}\left[a_{11}F(s) - f_w(x_7)\right] - a_7 x_5 + a_8 f(s)$ and $b_1(e_1) = -a_9$. With $e = (e_1, e_2)$, the terms $\Delta_1(e_1, t) = \bar{\Delta}_1 - \frac{1-s^*}{r}\bar{\Delta}_3$ and $\Delta_2(e, t) = \dot{x}_{6\delta} - a_{10}x_6$ are the system perturbations. It will be assumed that those perturbations and their first derivatives are bounded as $|\Delta_1(e_1, t)| \leq \Delta_1^+$, $\left|\dot{\Delta}_1(e_1, t)\right| \leq \Delta_1^+$, $|\Delta_2(e, t)| \leq \Delta_2^+$ and $\left|\dot{\Delta}_2(e, t)\right| \leq \Delta_2^+$.

Selecting

$$x_{6\delta} = -\frac{1}{b_1(e_1)}\left(f_1(e_1) + \lambda_1 e_0 + \lambda_2 e_1 - u_1\right) \tag{31}$$

as is [25], where $\dot{e}_0 = e_1$ and $\dot{u}_1 = -\alpha\psi_{1,2}(e_1, \dot{e}_1)$, with $\psi_{1,2} = \frac{\dot{e}_1 + |e_1|^{1/2}\text{sign}(e_1)}{|\dot{e}_1| + |e_1|^{1/2}}$ and $\alpha, \lambda_1, \lambda_2 > 0$, and applying the super-twisting control algorithm [12] as

$$u_b = \frac{1}{b_3}\left(u_{b_1} + u_{b_2}\right) \tag{32}$$

with $u_{b_1} = -k_{b_1}|e_2|^{1/2}\text{sign}(e_2)$, $\dot{u}_{b_2} = -k_{b_2}\text{sign}(e_2)$ and $k_{b_1}, k_{b_2} > 0$; the system (29)-(32) reduces to

$$\begin{cases} \dot{e}_0 = & e_1 \\ \dot{e}_1 = & -\lambda_1 e_0 - \lambda_2 e_1 + u_1 + b_1(e_1)\, e_2 + \Delta_1 \\ \dot{u}_1 = & -\alpha\frac{\dot{e}_1 + |e_1|^{1/2}\text{sign}(e_1)}{|\dot{e}_1| + |e_1|^{1/2}} \end{cases} \tag{33}$$

$$\begin{cases} \dot{e}_2 = & -a_{10}e_2 - k_{b_1}|e_2|^{1/2}\text{sign}(e_2) + \Delta_2 \\ \dot{u}_{b_2} = & -k_{b_2}\text{sign}(e_2) \end{cases} \tag{34}$$

where $\dot{e}_1$ is calculated applying a SM differentiator [19] and the brake valve is considered of the type of valve which can vary its position in a continuous range.

The stability of the closed loop system (33)-(34) is outlined in a step by step procedure. **Step A)** Reaching phase of the projection motion (34), **Step B)** Stability of the SM dynamics (33) and **Step C)** Stability of the zero dynamics x_7.

Step A) Let $q_b = u_{b_2} + \Delta_2(e, t)$, then from the equation (34), it follows that

$$\dot{e}_2 = -a_{10}e_2 - k_{b_1}|e_2|^{1/2}\text{sign}(e_2) + q_b \tag{35}$$

$$\dot{q}_b = -k_{b_2}\text{sign}(e_2) + \dot{\Delta}_2(e, t). \tag{36}$$

Under the assumption $\left|\dot{\Delta}_2(e, t)\right| \leq \Delta_2^+$, it follows that if $k_{b_1} > 0$ and $k_{b_2} > 3\Delta_2^+ + 4\left(\frac{\Delta_2^+}{k_{b_1}}\right)^2$, then $(e_2, q_b) = (0, 0)$ in finite time [23]. Establishing a SM in the manifold $e_2 = 0$ despite of the perturbation $\Delta_2(e, t)$.

Step B) Taking into account the equation (30) and defining $z_1 = e_1$ and $z_2 = \dot{e}_1$, the motion on the manifold $e_2 = 0$ is given by

$$\dot{z}_1 = z_2$$

$$\dot{z}_2 = -\lambda_1 z_1 - \lambda_2 z_2 - \alpha\frac{z_2 + |z_1|^{1/2}\text{sign}(z_1)}{|z_2| + |z_1|^{1/2}} + \dot{\Delta}_1(z_1, t)$$

Under the assumption $\left|\dot{\Delta}_1(e_1, t)\right| \leq \Delta_1^+$, it follows that if $\alpha > \Delta_1^+$, then $(z_1, z_2) = (0, 0)$ in finite time [26], establishing a SM on the manifold $e_1 = 0$ despite of the perturbation $\Delta_1(e_1, t)$.

Step C) Note that during braking process $x_7 > 0$ and with $s = s^*$ due to the control action, the zero dynamics becomes

$$\dot{x}_7 = -a_{11}F(s^*) - f_w(x_7) + \bar{\Delta}_3. \tag{37}$$

From the vehicle mechanics, the term $f_w(x_7) - \bar{\Delta}_3$ can be considered to be bounded $\left|f_w(x_7) - \bar{\Delta}_3\right| \leq \Delta_3^+$. In addition, $a_{11}F(s^*) \gg \bar{\Delta}_3$. Therefore, let $\gamma = a_{11}F(s^*) - \Delta_3^+$, $\gamma > 0$, and $V = \frac{1}{2}x_7^2$, then $\dot{V} = -x_7\left[a_{11}F(s^*) + f_w(x_7) - \bar{\Delta}_3\right] < -\gamma x_7$. Hence, $\dot{V} < -\gamma_0\sqrt{V}$, where $\gamma_0 = \gamma\sqrt{2}$. Thus, $x_7 = 0$ in finite time. Also, from (28) it follows that $x_5 = 0$ in finite time.

V. SIMULATION RESULTS

The feasibility of the proposed control scheme are shown in simulations on the wheel model design example, the system parameters are listed in Table 1.

TABLE 1
Values of Parameters (MKS Units)

Parameter	Value	Parameter	Value	Parameter	Value
m_c	1800	J	18.9	E	0.97
m_w	50	k_b	100	A_f	6.6
K_{cw}	1050	b_b	0.08	C_d	0.65
K_{wr}	175500	r	0.3	ρ	1.225
C_{cw}	19960	B	10	v_w	-6
C_{wr}	1500	C	1.9	g	9.81
τ	0.0043	D	1	v	0.5

To maximize the friction force, we suppose that slip tracks a constant signal during the simulations $s^* = 0.203$, which produces a value close to the maximum of the function $\phi(s)$. With parameters value presented in Table 1, the $\phi(s)$ function represents the friction relation under a dry surface condition.

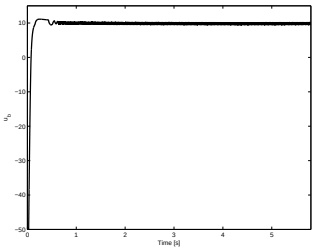

Fig. 3. Control signal for ABS u_b.

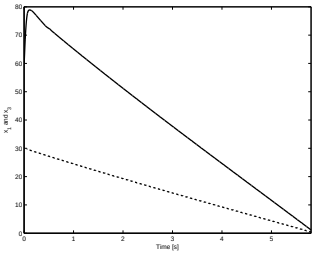

Fig. 4. Longitudinal speed x_7 (dashed) and the linear wheel speed x_5 (solid).

The road perturbation is considered as $z_r = 0.1\cos(10t)$. The control law parameters are, $k_{s_1} = 100000$, $k_{s_2} = 150000$, $K = \begin{bmatrix} -20 & 173 \end{bmatrix}^T$, $k_{b_1} = 1000$, $k_{b_2} = 500$, $\alpha = 100$ and $\lambda_1 = \lambda_2 = 50$. The matrix A is designed such that its eigenvalues are $\{-50, -60, -80 - 70\}$, while $\Lambda = 10000$ for HOSM observer design.

The control signal u_b for the ABS is presented in Fig. 3, and the longitudinal speed v and the linear wheel speed $r\omega$ are shown in Fig. 4, the ABS controller should be turned off when the longitudinal speed is close to zero.

The Figure 5 shows the slip rate during the breaking process. It can be observed the fast convergence to the reference value s^* and Fig. 6 presents the errors e_1 and e_2

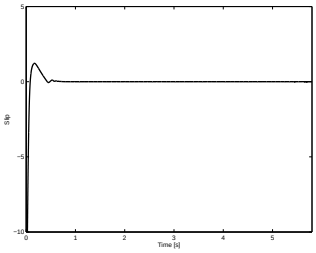

Fig. 5. Slip performance in the braking process.

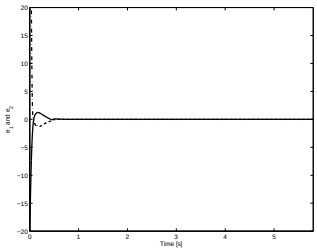

Fig. 6. Errors e_1 (solid) and, e_2 (dashed).

The Figure 7 shows the coordinate $\bar{x}_{11}$ position during the breaking process. The position is kept constant until the car is almost stopped. On the other hand, Fig. 8 shows the suspension position $\bar{x}_2$; it moves constantly, counteracting the changes on road and wheel.

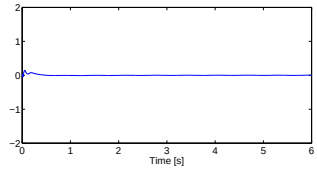

Fig. 7. Suspension position $\bar{x}_1$.

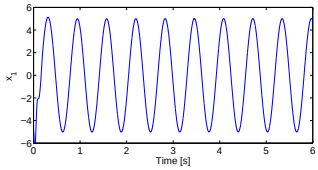

Fig. 8. Suspension position $\bar{x}_2$.

The control action u_s for the suspension is shown in Fig. 9. The valve can put or extract fluid into the reservoir to obtain the required force. The system arrives to the sliding surface (Fig. 10) and it is maintained there in spite of the unmatched perturbations coming from the road.

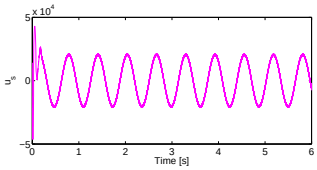

Fig. 9. Control signal for suspension u_s.

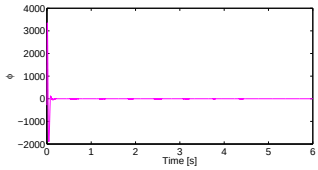

Fig. 10. Sliding surface σ.

VI. CONCLUSIONS

In this work HOSM based controllers for ABS assisted with active suspension has been proposed. In both cases, the simulation results of the closed-loop system are very accurate, taking into account the high uncertainty of the system, namely, parametric variations and neglected dynamics as well as the perturbations from the road.

REFERENCES

[1] H. Tan and Y. Chin, "Vehicle traction control: variable structure control approach," *Journal of Dynamic Systems, Measurement and Control*, vol. 113, pp. 223–230, 1991.

[2] C. Unsal and P. Kachroo, "Sliding mode measurement feedback control for antilock braking systems," *Control Systems Technology, IEEE Transactions on*, vol. 7, no. 2, pp. 271 –281, mar 1999.

[3] M. chin Wu and M. chang Shih, "Simulated and experimental study of hydraulic anti-lock braking system using sliding-mode PWM control," *Mechatronics*, vol. 13, no. 4, pp. 331 – 351, 2003.

[4] M. Tanelli, C. Vecchio, M. Corno, A. Ferrara, and S. Savaresi, "Traction control for ride-by-wire sport motorcycles: A second-order sliding mode approach," *Industrial Electronics, IEEE Transactions on*, vol. 56, no. 9, pp. 3347–3356, Sept. 2009.

[5] S. V. Drakunov, U. Ozguner, P. Dix, and B. Ashrafi, "ABS control using optimum search via sliding modes," *Control Systems Technology, IEEE Transactions on*, vol. 3, no. 1, pp. 79 –85, mar 1995.

[6] M. Tanelli, G. Osorio, M. di Bernardo, S. Savaresi, and A. Astolfi, "Limit cycles analysis in hybrid anti-lock braking systems," in *Decision and Control, 2007 46th IEEE Conference on*, Dec. 2007, pp. 3865–3870.

[7] Y. M. Sam, J. H. S. Osman, and M. R. A. Ghani, "A class of proportional-integral sliding mode control with application to active suspension system," *Systems & Control Letters*, vol. 51, no. 34, pp. 217 – 223, 2004.

[8] J. S. Lin and W. E. Ting, "Nonlinear control design of anti-lock braking systems with assistance of active suspension," *Control Theory Applications, IET*, vol. 1, no. 1, pp. 343 –348, january 2007.

[9] J. D. Sánchez-Torres, A. G. Loukianov, J. Ruiz-Leon, and J. Rivera, "ABS + active suspension control via sliding mode and linear geometric methods for disturbance attenuation," in *Decision and Control and European Control Conference (CDC-ECC), 2011 50th IEEE Conference on*, dec. 2011, pp. 8076 –8081.

[10] S. V. Drakunov and V. I. Utkin, "Sliding mode control in dynamic systems," *International Journal of Control*, vol. 55, pp. 1029–1037, 1992.

[11] V. I. Utkin, J. Guldner, and J. Shi, *Sliding Mode Control in Electro-Mechanical Systems*, ser. Automation and Control Engineering. CRC Press, 2009.

[12] A. Levant, "Sliding order and sliding accuracy in sliding mode control," *International Journal of Control*, vol. 58, no. 6, pp. 1247–1263, 1993.

[13] C. L. Clover and J. E. Bernard, "Longitudinal tire dynamics," *Vehicle System Dynamics*, vol. 29, pp. 231–259, 1998.

[14] P. A. Kruchinin, M. Magomedov, and I. V. Novozhilov, "Mathematical model of an automobile wheel for antilock modes of motion." *Mechanics of Solids*, vol. 36, no. 6, pp. 52–57, 2001.

[15] H. B. Pacejka, "In-plane and out-of-plane dynamics of pneumatic tyres," *Vehicle System Dynamics*, vol. 8, no. 4-5, pp. 221–251, 1981.

[16] E. Bakker, H. B. Pacejka, and L. Lidner, "A new tire model with application in vehicle dynamic studies," *SAE Paper No. 890087*, vol. 01, pp. 101–113, 1989.

[17] F. J. Bejarano and L. Fridman, "High order sliding mode observer for linear systems with unbounded unknown inputs," *International Journal of Control*, vol. 9, pp. 1920–1929, 2010.

[18] B. Molinari, "A strong controllability and observability in linear multivariable control," *Automatic Control, IEEE Transactions on*, vol. 21, no. 5, pp. 761 – 764, oct 1976.

[19] A. Levant, "Higher-order sliding modes, differentiation and output-feedback control," *International Journal of Control*, vol. 76, no. 9/10, pp. 924–941, 2003, special issue on Sliding-Mode Control.

[20] A. G. Louk'yanov and V. I. Utkin, "Method of reducing equations for dynamic systems to a regular form," *Automation and Remote Control*, vol. 42, no. 4, pp. 413–420, 1981.

[21] B. Draženović, "The invariance conditions in variable structure systems," *Automatica*, vol. 5, no. 3, pp. 287 – 295, 1969.

[22] A. Ferreira de Loza, E. Punta, L. Fridman, and G. Bartolini, "Output nested backward compensation of unmatched effects of unknown inputs," in *Decision and Control, 2010. CDC 2008. 40th IEEE Conference on*, dec. 2010, pp. 1448 –1453.

[23] J. A. Moreno and M. Osorio, "A Lyapunov approach to second-order sliding mode controllers and observers," in *Decision and Control, 2008. CDC 2008. 47th IEEE Conference on*, dec. 2008, pp. 2856 –2861.

[24] A. G. Loukianov, "Robust block decomposition sliding mode control design," *Mathematical Problems in Engineering*, vol. 8, no. 4-5, pp. 349–365, 2002.

[25] A. Estrada and L. Fridman, "Quasi-continuous HOSM control for systems with unmatched perturbations," *Automatica*, vol. 46, no. 11, pp. 1916 – 1919, 2010.

[26] A. Levant, "Quasi-continuous high-order sliding-mode controllers," *Automatic Control, IEEE Transactions on*, vol. 50, no. 11, pp. 1812 – 1816, nov. 2005.